

# Fluid-induced metamorphism and anatexis of refractory Ni-Co-Cu sulphides in subduction-related rocks

Nikita Kepezhinskas<sup>1,\*</sup>

<sup>1</sup>Department of Geolgocial Sciences, University of Florida, Gainesville, Florida, USA

**Abstract.** The role of metamorphism on refractory sulfides is not well constrained. Although experiments have displayed the effectiveness of high grade metamorphism, namely granulite facies metamorphism, on sulfide anatexis, its role in the presence of other variables is still poorly understood. Rocks from the Bay Islands Accretionary Complex in Honduras and the Ildeus-Lucha Complex in Russia exhibit extensive metamorphism. Sulfide mineralization is prolific in these rocks suggesting that metamorphism has played an important role in re-concentrating these sulfides during amphibolite and granulite facies metamorphism.

## 1 Overview

Magmatic Ni-Co-Cu sulfide deposits are typically associated with layered intrusions in continental rifts [1, 2]. They form in crustal magmatic conduits through multiple injections of metal-rich, mantle-derived mafic magma followed by advanced fractional crystallization and, in many cases, assimilation of sulfur-rich country rock [3-6]. Ni-Cu deposits at Aguablanca (Spain) suggest that metasomatic reactions are involved in the formation of refractory sulfide mineralization in orogenic environments [7]. Although amphibolite-facies sulfide metamorphism and anatexis is now well-documented in Pb-Zn-Cu-Ag ore at Broken Hill (Australia) and similar deposits [8-10], the importance of sulfide metamorphism and possible anatexis in refractory sulfide systems is very poorly understood.

Here, new data are presented for Ni-Co-Cu-PGE sulfide mineralization in subduction-related ultramafic rocks from northern Honduras and the Stanavoy mobile belt of Eastern Siberia. The role of post-magmatic transformation in these accretionary terranes and the mobility of refractory sulfides under these conditions form the main focus of this paper.

---

\* Corresponding author email: [nikitakep@ufl.edu](mailto:nikitakep@ufl.edu)

## 2 Metaultramafic rocks from the Black Rock Block, Bay Islands, Honduras

### 2.1 Geological Setting

The Bay Islands Accretionary Complex (BIAC) is an exhumed, accretionary terrane, which is located along the tectonically active, sinistral transform fault known as the Swan Islands – Motagua Fault Zone. This fault zone marks the boundary between the North American plate and the Caribbean plate and is thought to be a boundary along which subduction occurred in the Cretaceous [12-14]. The BIAC is composed of a wide amalgamation of fault-bounded metasedimentary, metamorphic, and metaigneous blocks and rock units. The extent of metamorphism in these blocks is varied, with some rocks preserving relics of granulite and amphibolite-facies metamorphism and with all the rocks exhibiting a greenschist-facies overprint of original metamorphic fabric. On the northwestern end of the island of Guanaja, (Figure 1) one such accretionary block, known as the Black Rock Accretionary Block (BRAB), is preserved and composed of granite, serpentinite, hornblendite, metadacite and gneiss.

### 2.2 Petrology and geochemistry of metaultramafic units

As with the rest of the BIAC, the metaultramafic units of the BRAB have undergone extensive metamorphism. Metapyroxenites are characterized by Nb-Ta depletions and are interpreted as arc-related ultramafic cumulates. The serpentinites are the most far removed from their protolith, and are dominated by serpentinite group minerals with distinctive greenish-blue coloration and asbestiform texture.

The hornblendites of the BRAB are defined by two groups: biotite hornblendites and biotite pyroxenites. The major mineral phases that make up the biotite hornblendites are biotite + Mg-hornblende + actinolite. The major phases that make up the biotite pyroxenites are biotite + diopside + hornblende.

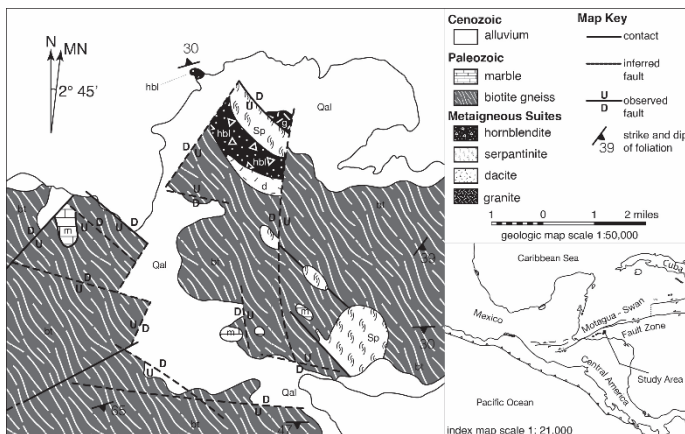


**Fig. 1.** Detailed geologic map of the BRAB block on the island of Guanaja, Honduras.

#### 2.2.1 Biotite

Large biotite, up to 6 cm long, is prevalent among the BRAB hornblendites and pyroxenites. Crystals are brown in parallel nicols and crossed nicols and display

characteristic birds-eye extinction in crossed nicols. A few crystals of the biotite are replaced by chlorite, a greenish mineral with anomalous birefringence.

### 2.2.2 Amphibole

Amphibole from the BRAB hornblendites and pyroxenites can be grouped into two groups (Figure 2a). The first group is characterized by a periwinkle blue to tan pleochroism and

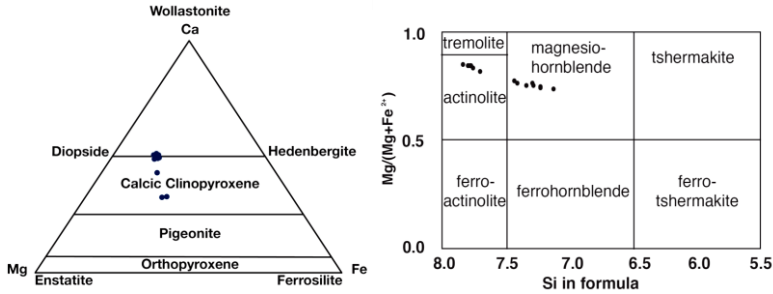


**Fig. 2.** Discrimination diagram for BRAB pyroxenes (left) and discrimination diagram for BRAB pyroxenes (right).

pronounced amphibole cleavage. This group is characterized by high Mg and low Si in the amphibole formula. The second, less abundant group is teal to green pleochroic and has more Si in the amphibole formula. Much of the amphibole is replaced by chlorite, a greenish mineral with anomalous birefringence.

### 2.2.3 Pyroxenes and inclusions

Pyroxene from the BRAB hornblendites and pyroxenites is characterized by low birefringence and characteristic pyroxene cleavage. Inclined extinction and an abundant Ca content (Figure 2b) identify the pyroxene minerals in these rocks as diopside and augite clinopyroxenes. Of particular note are several spheroidal and dumbbell-like trails of sulfide inclusions in these clinopyroxenes. Although the inclusions seem to be heterogeneous, analysis reveals that many inclusions have chalcopyrite, pyrrhotite and Co-pentlandite affinities. In some case, all three phases can be present in the same inclusion. These inclusions are emplaced along three main trends and are around 4 to 6 inclusion-trail lines wide (Figure 3).

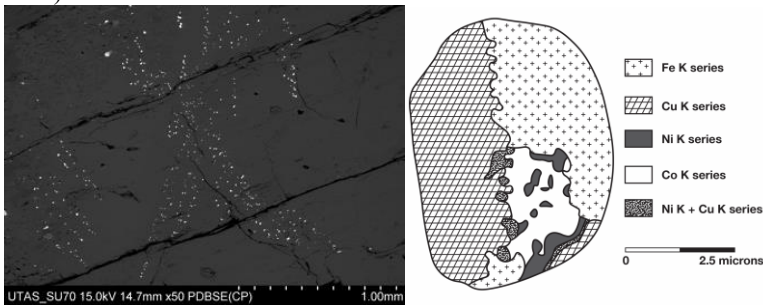


**Fig. 3.** Back-scatter electron image of sulphide inclusion trails in diopside (left) and schematic EDX map of one sulphide melt inclusion (right).

## 3 Ultramafic rocks from Ildeus-Lucha complex (Stanovoy Super-Terrane, Russia)

### 3.1 Geological Setting

The Central Asian Orogenic Belt (CAOB) is a long-lived mobile belt system spanning the Proterozoic to the Triassic [15]. The Ildeus-Lucha ultramafic-mafic complex (ILC) is emplaced in the crust of the Stanovoy arc (Figure 4), a mobile belt in the CAOB and dates to about 233 Ma [16]. The rocks of the ILC were likely metamorphosed at greenschist to amphibolite facies metamorphism around 140 Ma and later intruded by post-collision adakites and shoshonitic lamprophyres around 117-115 Ma [16].

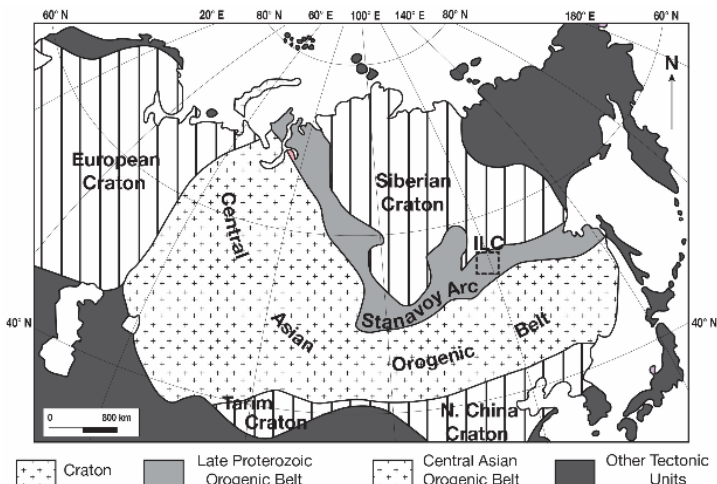


**Fig. 4.** General tectonic map of the CAOB [15] and location of the Ildeus-Lucha Complex (ILC).

### 3.2 Petrology and Geochemistry

Pronounced enrichment in large-ion lithophile (Cs, Rb, Ba, Sr, U) and depletion in high-field strength (Nb, Ta, Zr) elements in ILC rocks suggest derivation from a subduction-related source [16]. The ILC is composed of dunite, wehrlite, pyroxenite and gabbro. Main minerals include Mg-rich olivine with extremely low Al, Ca and high Mn contents and pargasite along with serpentine, tremolite and chlorite and relics of magmatic clino- and orthopyroxenes. Changes in metamorphic mineralogy possibly reflect transition from subduction-related greenschist to collision-related amphibolite metamorphism in the lower arc crust [17]. ILC rocks contain abundant pentlandite, Co-pentlandite (7-16 wt.% CoO), chalcopyrite, bornite, hazelwoodite, digenite, Ni-pyrite, Ni-sphalerite and a Co-Cu sulfide. Pargasitic amphibole contains inclusions of K-Br-I-Cl salts (Figure 5A), while biotite contains abundant Cl-F-apatite (Figure 5B).

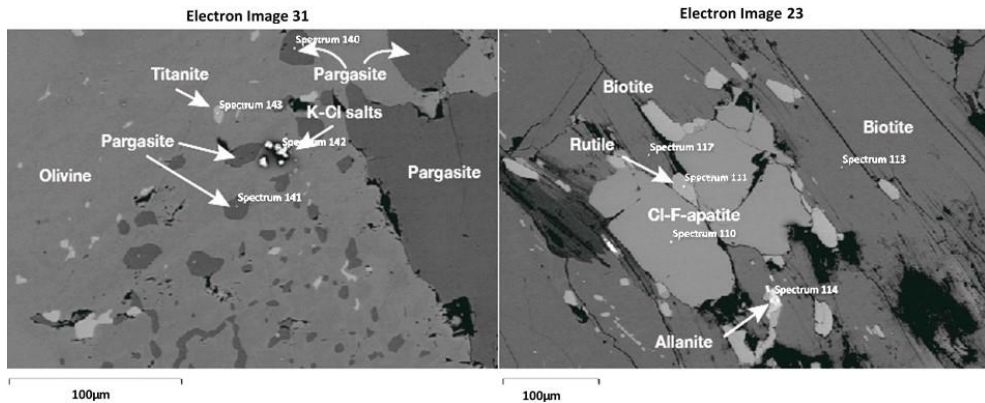


**Fig. 5.** General tectonic map of the CAOB [15] and location of the Ildeus-Lucha Complex (ILC).

## 4 Overview

Refractory sulfide deposits in Phanerozoic mobile belts and accreted terranes were impacted by greenschist to amphibolite-facies metamorphism resulting in chemical, mineralogical and textural changes in sulfide mineralization [7, 16]. Droplet-shaped sulfide inclusions in silicates associated with Pb-Zn-Ag ore at the Broken Hill deposit suggest large-scale sulfide anatexis under amphibolite-facies conditions [8, 9], although exact mechanism of such low-temperature melting of sulfide minerals is not well understood due to apparent lack of applicable experimental and thermodynamic data [10, 11]. Melt inclusions in meta-ultramafic rocks from Guanaja are composed of chalcopyrite, pyrrhotite and Co-pentlandite, all of which are refractory sulfides with higher melting temperatures compared to Pb-Zn sulfide systems. It was suggested that presence of multiple sulfide phases may substantially lower sulfide cotectic temperature to allow melting under peak amphibolite facies conditions (4-5 kbars, 550°C) [10]. We suggest that melting of refractory sulfides can be further facilitated by involvement of Cl-rich aqueous fluids. Presence of abundant amphibole, biotite and Cl-F-apatites in subduction-related ultramafic rocks from Guanaja and Stanovoy Belt as well as occurrence of K-Cl salts and Cl-F-apatites in Stanovoy rocks suggests fluid-saturated conditions during their metamorphism and sulfide anatexis. It is proposed that these processes may possibly play important role in the formation of refractory Ni-Co-Cu sulfide mineralization in subduction-related environments such as Phanerozoic orogenic belts and accretionary terranes in modern arcs.

I thank Drs. D.Foster, G.Kamenov, V.Kamenetsky and P.Kepezhinskas for their constant support and advice during this work. I also acknowledge financial and logistical support from PNK GeoScience (Tampa, USA) during my fieldwork in Guanaja (Honduras) and from Khingan Minerals AS (Oslo, Norway) during my stay at the University of Tasmania (Hobart, Australia).

## References

1. N.T. Arndt, C.M. Leshner, G.K. Czamanske, *Econ. Geol.*, **100**, 5-24 (2005)
2. A.J. Naldrett, *Econ. Geol.*, **105**, 669-688 (2010)
3. R.R. Keyas, P.C. Lightfoot, *Mineral. Deposita*, **45**, 241-257 (2010)
4. E.M. Ripley, C. Li, *Econ. Geol.*, **108**, 45-58 (2013)
5. P.C. Lightfoot, D.M. Evans-Lamswood, *Ore Geol. Rev.*, **64**, 354-386 (2015)

6. S.J. Barnes, D.A. Holwell, M. Le Vaillant, *Elements*, **13**, 89-95 (2017)
7. R. Piña, I. Romeo, L. Ortega, R. Lunar, R. Capote, F. Gervilla, C. Quesada, *Geol. Soc. Amer. Bull.*, **122**, 915-925 (2010)
8. B.R. Frost, J.A. Mavrogenes, A.G. Tomkins, *Can. Mineral.*, **40**, 1-18 (2002)
9. H.A. Sparks, J.A. Mavrogenes, *Econ. Geol.*, **100**, 773-779 (2005)
10. A.G. Tomkins, D.R.M. Pattison, B.R. Frost, *J. Petrol.*, **48**, 511-535 (2007)
11. P.G. Spry, I.R. Plimer, G.S. Teale, *Ore Geol. Rev.*, **34**, 223-241 (2008)
12. M.R. Perfit, B.C. Heezen, *Bull. Geol. Soc. Amer.*, **89**, 1155-1174 (1978)
13. R.D. Rogers, P. Mann, *Geol. Soc. Amer. Spec. Paper*, **428**, 37-64 (2007)
14. L. Ratschbacher et al., *Geol. Soc. London, Spec. Publ.*, **328**, 219-293 (2009)
15. A. Kröner et al., *Gondwana Res.*, **25**, 103-125 (2014)
16. P.K. Kepezhinskas, N.P. Kepezhinskas, V.S. Kamenetsky, N.V. Berdnikov, *Geol. Soc. Amer. Abstr. Progr.*, **50**, doi: 10.1130/abs/2018AM-320293 (2018)